Desalination and Water Treatment
www.deswater.com

doi:10.5004/dwt.2021.27145

225 (2021) 430–442
June

Low-cost biosorbents from pines wastes for heavy metals removal from wastewater: adsorption/desorption studies.

Manel Touihri[a], Susana Gouveia[b], Fatma Guesmi[a], Chiraz Hannachi[a], Béchir Hamrouni[a], Claudio Cameselle[b,*]

[a]*Laboratory of Desalination and Water Treatment LR19ES01, Faculty of Sciences of Tunis, University of Tunis, EL Manar, 2092, Tunis, Tunisia, emails: manel.touihri@fst.utm.tn (M. Touihri), guesmi_fatma@yahoo.fr (F. Guesmi), chiraz.hannachi@fst.utm.tn (C. Hannachi), bechir.hamrouni@fst.utm.tn, (B. Hamrouni)*
[b]*BiotecnIA, Department of Chemical Engineering, University of Vigo, Rua Maxwell s/n, Building Fundicion, 36310 Vigo, Spain, ORCID: 0000-0003-4785-1585, Researcher ID: F-3363-2014, Tel. +34 986812318; Fax: +34 986812201; emails: claudio@uvigo.es (C. Cameselle), gouveia@uvigo.es (S. Gouveia)*

Received 24 January 2020; Accepted 21 December 2020

ABSTRACT

The use of inexpensive materials such as agricultural by-products and industrial waste has received considerable attention because of their high efficiency for heavy metal retention, low cost and availability. This study aimed to investigate the technical feasibility of residual biomass from pines (cones and leaves) for Cr(VI) and Cu(II) removal from aqueous solutions. The effect of various parameters, such as pH, metal concentration, contact time, temperature and biosorbent/solution ratio was examined. Biosorbents were characterized using scanning electron microscopy combined with energy-dispersive X-ray spectroscopy and Fourier-transform infrared spectroscopy. The specific surface area was evaluated by the Brunauer–Emmett–Teller isotherm. The equilibrium data showed better fitting to the Langmuir model, indicating the monolayer adsorption behavior. The Langmuir model predicted a maximum adsorption capacity of 27.78 mg g^{-1} of Cu(II) on pine cones and 64.04 mg g^{-1} of Cr(VI) on pine leaves. The kinetic study revealed that the pseudo-second-order model fitted the experimental data. The thermodynamic study showed that the biosorption process was endothermic for Cu and exothermic for Cr(VI). The biosorbent can be reactivated with 0.1 mol L^{-1} HNO_3 allowing the recovery of the metals and the recycling of the biosorbent. These results showed that pine waste materials can be used as efficient, economic and eco-friendly biosorbent for Cu(II) and Cr(VI) recovery from contaminated effluents.

Keywords: Biosorption; Desorption; Langmuir isotherm; Pine biomass; Chromium; Copper

1. Introduction

Water pollution by heavy metals is one of the major environmental issues around the globe that have received widespread attention due to the high toxicity of most metallic species on aquatic organisms and the potential risk for human health. The origin of heavy metal contamination is often associated with various mining and industrial activities, as well as the lack of an appropriate waste management system. Heavy metals are commonly detected in wastewater from the mining and electroplating industries, smelting and petroleum refining, tanneries and battery manufacture [1–4]. Metals are non-biodegradable in nature and they can be persistently accumulated in the food chain, thus

* Corresponding author.

posing a serious threat to the health of living organisms and the natural environment as a whole [5–7].

Among various heavy metals, chromium is recognized to be highly toxic. Chromium exists in several oxidation states (from –2 to +6) but the most stable form is the trivalent cation (Cr^{3+}) and the hexavalent anions (chromate and dichromate). Compared to Cr(III), Cr(VI) is more mobile, bioavailable and, hence more toxic. It is considered carcinogenic and mutagenic for most organisms [8]. Human exposure to chromium may cause several diseases such as liver damage, allergic skin reactions, bronchitis and bronchogenic carcinoma [9,10]. Copper (Cu) has been considered as one of the most harmful ions, especially when its concentration exceeds the maximum contamination level of 1.3 mg L^{-1} (USEPA, 2009). Acute exposure to large doses of Cu is associated with several diseases like kidney damage, pancreas and heart diseases, gastrointestinal irritation and it increases the risk of lung cancer [11,12]. Thus, the removal of these metal ions from wastewater prior to its discharge into natural water is of utmost interest.

Several conventional processes such as solvent extraction [13], flotation [14], coagulation [15], electrochemical treatment [16], ion exchange [17] and membrane separation [18] have been tested and implemented for removing heavy metals from industrial effluents. However, the application of these technologies is limited by their high cost and complicated operation, inefficiency at low concentrations and the generation of toxic wastes.

Biosorption stands out as a potent alternative technology given to its low cost, ease of operation, high efficiency, even at low metal concentration, no formation of chemical wastes, and the possibility of recycling the adsorbent [19–21].

In the last few decades, several research works have been devoted to looking for promising cost-effective adsorbents. Agricultural wastes have been recognized as an important source of promising biosorbents due to its good retention capacity, availability, low cost, and the possibility of their regeneration and reuse [3,22]. Heavy metals are retained in the biosorbents by binding through functional groups such as carbonyl, phenolic, amino, etc. [7,23]. Various biosorbents produced from agricultural wastes were efficiently used for heavy metals recoveries such as rice husk [24], peanut shell [25], banana peel [26], olive stones [27] and sawdust [28].

The aim of this work is to investigate the potential capacity of pine waste materials, that is, pine leaves and pine cones, as biosorbents for removing chromium (VI) and copper (II) from synthetic wastewater. The influence of various variables in the adsorption process was studied: metal concentration, adsorbent dose, pH, contact time and temperature. The adsorption isotherm as well as the adsorption kinetics and the thermodynamic behavior were investigated. The surface morphology of the biosorbents was determined by scanning electron microscopy/energy-dispersive X-ray spectroscopy (SEM/EDS). The possible functional groups and the potential binding sites were evaluated by Fourier-transform infrared spectroscopy (FTIR) analysis. The specific surface area was evaluated by the Brunauer–Emmett–Teller (BET) isotherm. Desorption studies on the pine waste materials were performed to determine the possibility of regeneration and reuse of the biosorbent.

2. Materials and methods

2.1. Chemicals and analytical methods

Potassium dichromate ($K_2Cr_2O_7$), copper(II) sulfate pentahydrate ($CuSO_4{\cdot}5H_2O$), and ethylenediaminetetraacetic acid (EDTA) were purchased from Sigma-Aldrich (Spain). Other chemicals used were of analytical grade and supplied by Panreac (Spain). Stock solutions (1 g L^{-1}) of chromium and copper were prepared by dissolving the required amount of $K_2Cr_2O_7$ or $CuSO_4{\cdot}5H_2O$ in 1 L of deionized (DI) water. Working concentrations ranging from 10 to 1,000 mg L^{-1} were prepared by dilution of the stock solutions. The pH of the metal solutions was measured with a CyberScan PC 510 pH-meter (Eutech Instruments, USA). The pH was adjusted when necessary by adding hydrochloric acid (HCl, 0.1 mol L^{-1}) or sodium hydroxide (NaOH, 0.1 mol L^{-1}). The concentration of Cu(II) and Cr(VI) in the solutions was determined by inductively coupled plasma–optical emission spectrometry (ICP-OES) at the Analysis Center CACTI of the University of Vigo. The concentration of Cr(VI) was determined by UV-Vis spectrophotometry at 540 nm with the 1,5-diphenylcarbazide method. The reagent 1,5-diphenylcarbazide form a violet complex with Cr(VI) which is then measured in a spectrophotometer at 540 nm.

2.2. Adsorbents preparation

Pine tree cones and leaves were collected from the area of the University of Tunis, El Manar, Tunis (NW Tunisia). They were washed with distilled water to remove impurities, and dried in an oven at 70°C for 24 h. Dried biomass was grounded and passed through a sieve of 150 μm size. The fraction smaller than 150 μm was collected and stored in an airtight plastic container for future using.

2.3. Adsorbent characterization

The surface morphology of the two absorbents was observed by SEM combined with an EDS analyzer (Thermo Scientific™ Quanta™ 200 SEM) with an accelerating voltage of 20 kV. FTIR spectra before and after the biosorption tests were measured by the Perkin Elmer Spectrum 100 analyzer over the 4,000–400 cm^{-1} wavenumber range. Samples were prepared using the KBr pellet method. Specific surface area, particle size, and pore diameter were measured from the N_2 adsorption/desorption isotherm at 100°C using ASAP 202 (Micromeritics, USA) apparatus. The pH at point of zero charge (pH_{pzc}) of the prepared sorbents was estimated by the salt addition method [29]. In a series of 100 mL Erlenmeyer flasks, 0.15 g of pine cones (PC) or pine leaves (PL) powders were dispersed in 50 mL of NaCl solution (0.01 mol L^{-1}). The initial pH (pH_i) of NaCl solution was fixed in the range of 2–12. The mixture was vigorously stirred for 24 h and the final pH (pH_f) was measured. The isoelectric point is the intersection between the bisector and the plot of pH_i vs. pH_f.

2.4. Adsorption Experiment

Batch adsorption experiments were performed in 50 mL Erlenmeyer flasks adding 0.4 g of biosorbent to 40 mL of

solution of the target heavy metal ion (Cr(VI) or Cu(II)). The mixture was kept under agitation at a constant temperature (20°C) using an orbital shaker with agitation and temperature control (CORNING LSE 49 L) until the adsorption equilibrium was reached. The biosorbent suspensions were filtered through filter paper. Filtrates were collected and analyzed for residual metal concentration.

The effects of adsorbent dose (0.1–1.2 g), initial concentration of metal (10–1,000 mg L^{-1}) and pH (1–10) on the adsorption process were investigated. Kinetic study and the effect of contact time were carried out for 48 h and the results were fitted to pseudo-first-order, pseudo-second-order and intraparticle diffusion models. The effect of temperature and thermodynamic study were carried out in the range of 10°C–60°C. The amount of metal adsorbed in the equilibrium q_e (mg g^{-1}) was evaluated using Eq. (1).

$$q_e = \frac{\left(C_0 - C_e\right)V}{W} \tag{1}$$

where C_0 (mg L^{-1}) is the initial metal concentration in the liquid phase, C_e (mg L^{-1}) is the metal concentration in the equilibrium in the liquid-phase, V is the volume of the liquid phase (L), and W is the adsorbent dose (g).

2.5. Desorption experiments

A desorption study was carried out to regenerate/recycle the biosorbent used for copper and chromium adsorption. The experiments were conducted using different reagents: HNO_3, HCl, EDTA, NaOH (0.1 mol L^{-1}) and deionized water. The metal-loaded biosorbent was mixed with 40 mL of each regeneration solution and shaken at 180 rpm and 20°C overnight. Then, the liquid phase was separated by filtration and analyzed for metal (Cr(VI) or Cu(II)) concentration. The biosorbent was collected, washed with DI water and reused in a new biosorption process. The desorption ratio was evaluated using Eq. (2).

$$\text{Desorption ratio} = \frac{\text{amount of metal ion desorbed}}{\text{amount of metal ions adsorbed}} \tag{2}$$

3. Results and discussion

3.1. Characterization of the adsorbents

3.1.1. SEM, EDS and BET analysis

The morphology of pine cones (PC) and pine leaves (PL) was investigated by SEM. Fig. 1a–c revealed that PC biomass has a relatively smooth surface structure with fibrillary packing. The external surface of pine leaves showed a rough and coarse morphology with some wrinkles and pores (Fig. 1e–g). After Cu adsorption, the PC surface appeared with some scars which may be related to the deposition of copper on the surface (Fig. 1d). The surface of pine leaves after Cr(VI) loading has not significantly changed.

The elemental composition of prepared sorbents before and after heavy metal sorption was investigated and the results are shown in Fig. 2. The EDS detected the main elements in pine cones being the most abundant element carbon (76.90% wt.), followed by oxygen (27.55% wt.), aluminum (0.97% wt.), calcium (0.39% wt.) and silicon (0.18% wt.) (Fig. 2a). Elemental composition analysis of PL surface revealed the presence of C, O, Na, Mg, Si, S, Cl, K and Ca (Fig. 2c). The adsorption of Cu(II) and Cr(VI) onto PC and PL was confirmed by EDS results as shown in Fig. 2b and d.

The physical properties, that is, surface area, pore volume and pore size of PC and PL have been investigated. The results showed that the BET surface area, the pore volume and the average pore size were 5.50 $m^2\ g^{-1}$, 0.0104 $cm^3\ g^{-1}$ and 10.84 nm respectively for the pine cones. BET surface area of PL was found to be 3.04 $m^2\ g^{-1}$, pore volume and pore size of PL were 0.0027 $cm^3\ g^{-1}$ and 7.23 nm, respectively.

3.1.2. FTIR analysis

FTIR analysis was performed to reveal the functional groups of the biosorbent surface and to identify their interaction with metal ions. Fig. 3 shows FTIR spectra analyses of PC and PL before and after adsorption of Cu(II) or Cr(VI). Fig. 3a (PC spectra) revealed a broadband at 3,335.64 cm^{-1} assigned to hydroxyl (–OH) or amine (–NH) groups. The peak at 2,926 cm^{-1} corresponds to the stretching vibration bands of the C–H groups. The band at 1,604.13 cm^{-1} is characterized by the stretching vibration of a carboxyl group (–COOH). The peaks at 1,263.41 and 1,024.21 cm^{-1} corresponds to the stretching vibrations of the CO group. The band observed at 667.83 cm^{-1} may be related to C–Cl group. These results indicated the presence of some functional groups such as hydroxyl, carboxyl and amino on PC surface. The FTIR spectra of the Cu-loaded PC showed that the peaks expected at 3,335.9; 2,930.0; 1,613.9; 1,263.4 and 1,026.4 cm^{-1} have shifted to 3,325.5; 2,929.3; 1,621.0; 1,264.9 and 1,024.9 cm^{-1}, respectively. These changes suggest that the corresponding functional groups (–OH, –NH, –COOH, CO) may be involved in Cu adsorption.

In the case of pine leaves (Fig. 3b), the stretching vibration band of –OH, –NH, –COOH, and CO functional groups had shifted to 3,327.6; 2,920.1; 1,613.6 and 1,029.4 cm^{-1}. Similarly, it is assumed that these functional groups may be involved in the biosorption of Cr(VI).

3.1.3. Determination of the pH of point zero charge

The pH_{pzc} estimated for PC and PL was found to be 6.6 and 4.4 respectively (Fig. 4). For pH < pH_{pzc} the active sites of the adsorbent are protonated and have a positive charge. However, pH > pH_{pzc}, the surface charge of the adsorbent is negative [30]. The charge of the solid surface will have an impact in the adsorption of cations or anions. It is hypothesized that Cu will be more effectively adsorbed at pH above the pH_{pzc}, whereas dichromate anions will be preferably adsorbed at pH below the pH_{pzc}.

3.2. Selection of adsorbent

Pine waste materials (cones and leaves) were tested as adsorbents for the removal of Cu(II) and Cr(VI) (Fig. S1). Higher removal of Cu(II) was achieved with pine cones. About 76% of the initial Cu(II) was removed with PC whereas PL retained only 13% of Cu(II). Cr(VI) showed

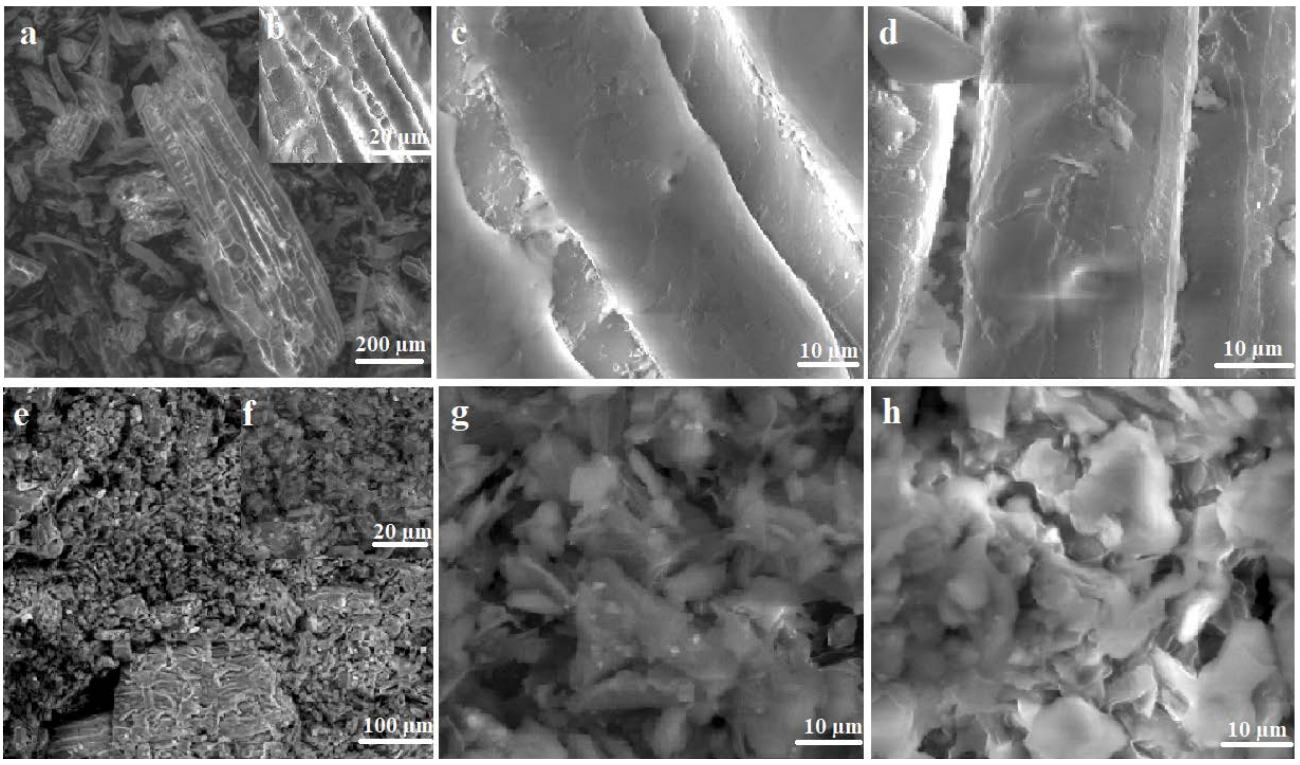

Fig. 1. SEM of pine cones samples: before Cu(II) adsorption (a) magnification x 150, (b) magnification: x 1000, (c) magnification: x 2500; after Cu(II) adsorption at initial concentration of 250 mg L^{-1} (d) magnification x 2500. SEM of pine leaves samples: before adsorption (e) magnification x 300, (f) magnification x 1000, (g) magnification x 2500; after Cr(VI) adsorption at initial concentration of 250 mg L^{-1} (h) magnification x 2500.

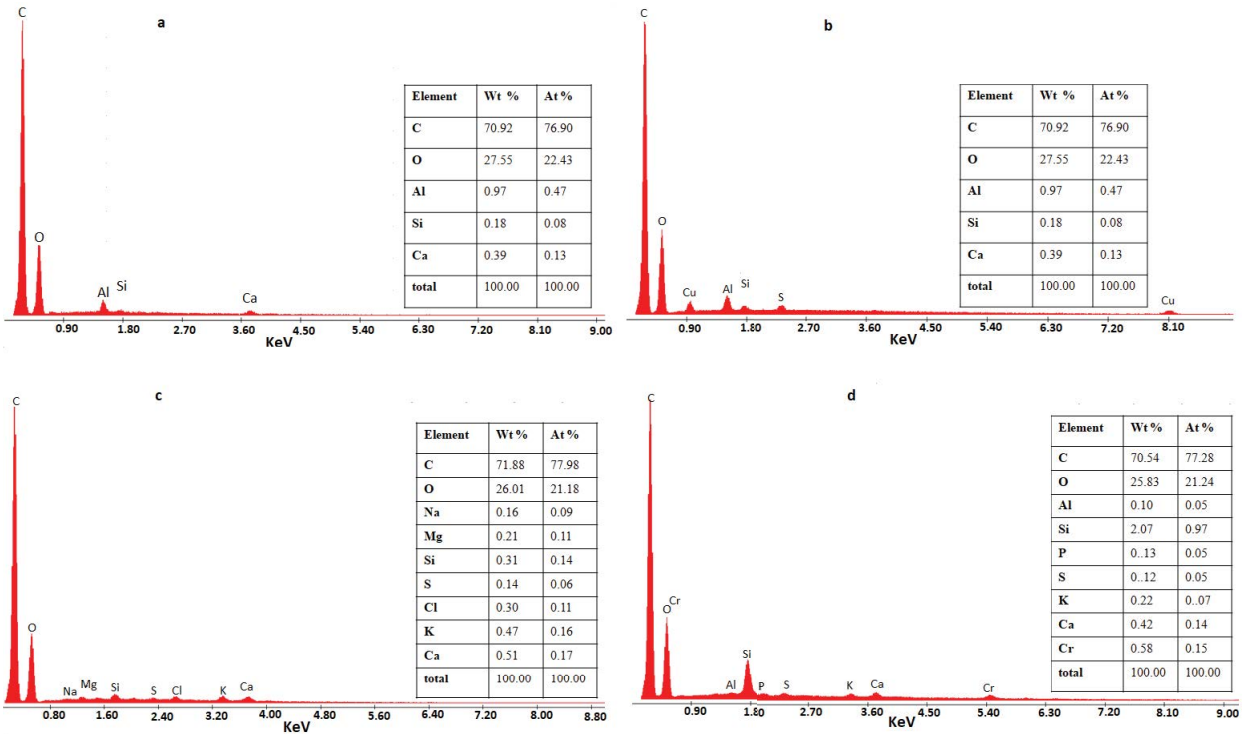

Element	Wt %	At %
C	70.92	76.90
O	27.55	22.43
Al	0.97	0.47
Si	0.18	0.08
Ca	0.39	0.13
total	100.00	100.00

Element	Wt %	At %
C	70.92	76.90
O	27.55	22.43
Al	0.97	0.47
Si	0.18	0.08
Ca	0.39	0.13
total	100.00	100.00

Element	Wt %	At %
C	71.88	77.98
O	26.01	21.18
Na	0.16	0.09
Mg	0.21	0.11
Si	0.31	0.14
S	0.14	0.06
Cl	0.30	0.11
K	0.47	0.16
Ca	0.51	0.17
total	100.00	100.00

Element	Wt %	At %
C	70.54	77.28
O	25.83	21.24
Al	0.10	0.05
Si	2.07	0.97
P	0..13	0.05
S	0..12	0.05
K	0.22	0..07
Ca	0.42	0.14
Cr	0.58	0.15
total	100.00	100.00

Fig. 2. Energy spectrum by EDS of: (a) pine cones before adsorption, (b) pine cones after Cu(II) at an initial concentration of 250 mg L^{-1}, (c) pine leaves before Cr(VI) adsorption and (d) pine leaves after Cr(VI) adsorption at an initial concentration at 250 mg L^{-1}.

different behavior. Pine leaves were much more effective retaining Cr(VI) (87% of the initial chromium was adsorbed) than pine cones, which retained only 44% of the initial chromium. Thus, PC was selected in this study for the adsorption of Cu(II) whereas PL was used as an adsorbent for Cr(VI).

3.3. Adsorption of Cu(II) and Cr(VI) in batch tests

3.3.1. Effect of pH

pH solution is one of the most important parameters for adsorption since it has a critical influence on heavy metal speciation and binding to the solid surface of the adsorbent. pH affects the properties of the adsorbate and adsorbent, such as the surface charge and the ionic state of functional groups in the adsorbent, and the speciation of the adsorbate [31]. The effect of pH on Cr(VI) adsorption was studied in the range from pH = 1 to 10, whereas Cu(II) adsorption was studied from pH = 1 to 8 due to the lack of stability of Cu(II) in alkaline solutions.

As depicted in Fig. 5a, the adsorbed Cu(II) increased from 20% to 98% when the pH increased from pH 2 to 6.4. This can be interpreted in terms of the activity of the hydronium ions (H_3O^+). At low pH, H_3O^+ will compete with metal ions for the active sites. Most of the biosorbent sites would be occupied by protons resulting in an increase in positive charges on the adsorbent surface. Thus, repulsive forces will be created, which in turn, reduce copper sorption. As pH increases, the concentration of H_3O^+ decreases, resulting in an increasing amount of negative charges on the surface. Thus, the interaction between Cu(II) and

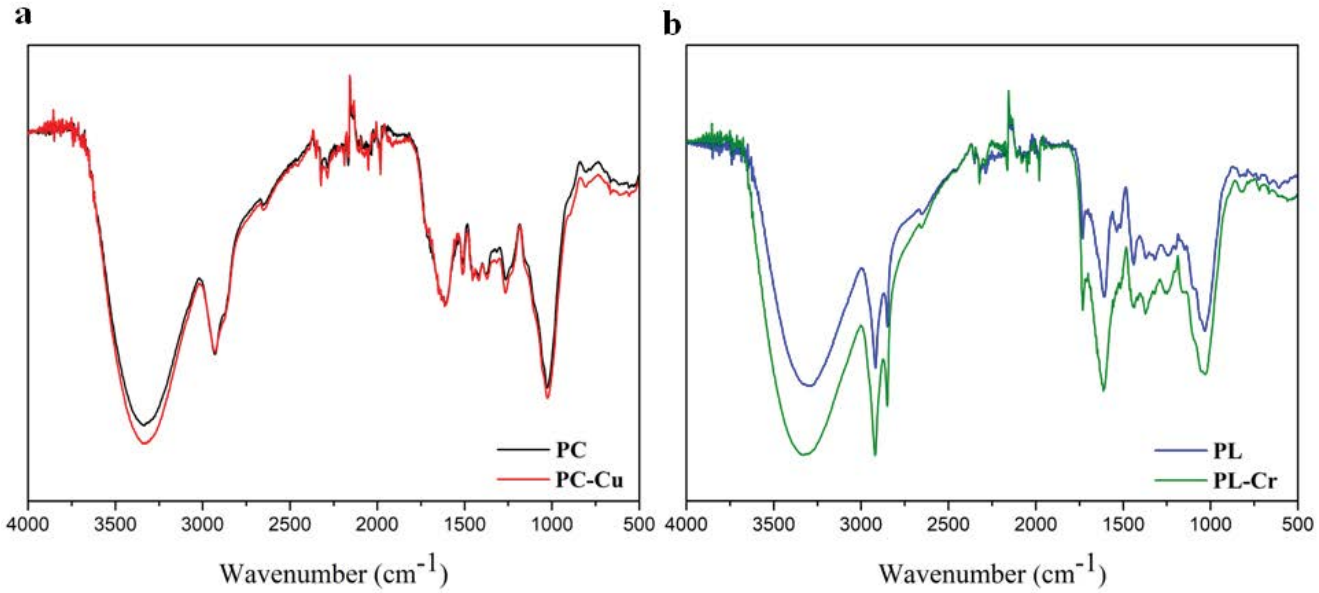

Fig. 3. FTIR spectra of the two adsorbents before and after metal adsorption. (a) Cu(II) with pine leaves and (b) Cr(VI) with pine cones.

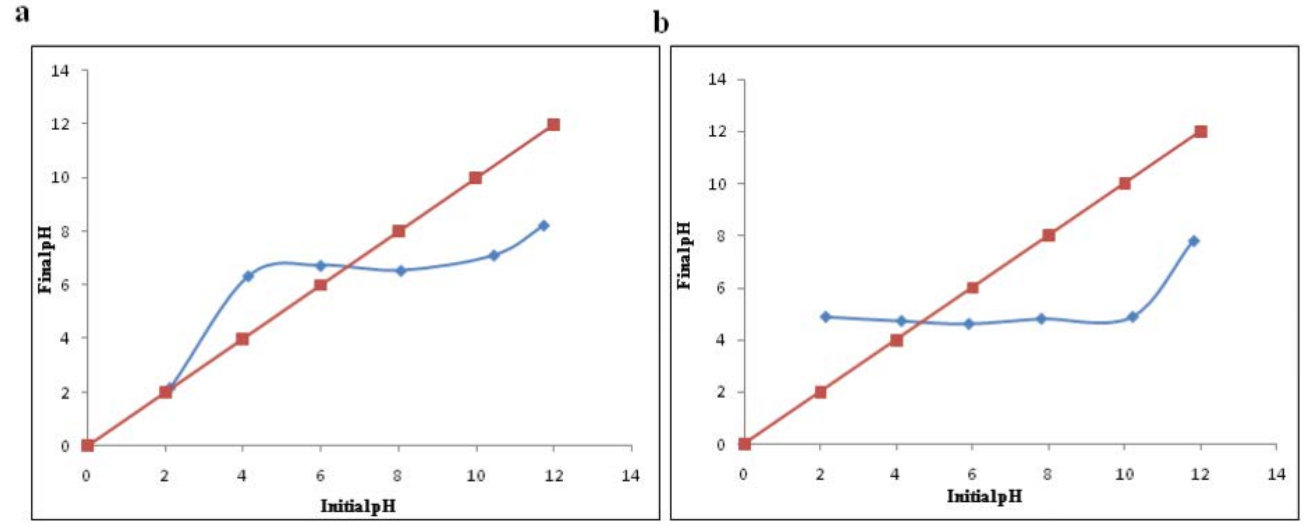

Fig. 4. Determination of the pH at the point of zero charge for the sorbents: (a) pine cones and (b) pine leaves.

binding sites increases, which results in higher Cu(II) removal from the solution [21,32,33]. This was also confirmed by the pH_{pzc} since the estimated value was 6.6 and below this pH, the surface of pine cones was positively charged thus, Cu(II) sorption was not favored. For pH higher than 6.6, pine cones surface was negatively charged favoring Cu(II) sorption by electrostatic attraction. At pH above 6, there is a decrease in adsorption capacity due to the precipitation of copper as $Cu(OH)_2$ [34]; thus, copper ions are not available in the solution to be adsorbed onto PC.

In the tests with chromium, the adsorption capacity increases up to pH 6, and then decreases from pH 6 to 10. Maximum Cr(VI) adsorption (88.5%) was achieved at pH 6 (Fig. 5a). Cr(VI) exists in different forms: H_2CrO_4, $HCrO_4^-$, CrO_4^{2-}, and $Cr_2O_7^{2-}$ depending on the pH of the solution. At low pH, the predominant forms are $HCrO_4^-$ and $Cr_2O_7^{2-}$. As the pH increases, the predominant form shifts to CrO_4^{2-}. As a result, the divalent CrO_4^{2-} ion is the dominant species in alkaline conditions [35–37].

In acidic solutions, the surface of the adsorbent is protonated acquiring positive charges, favoring the electrostatic attraction between the negatively charged ions (chromate and dichromate) and the binding sites. In addition, lower pH favors the binding of $HCrO_4^-$ to acidic functional groups. Therefore, Cr(VI) adsorption was enhanced at low pH [9,38]. Similar behavior of Cr(VI) adsorption has been also reported in the literature [39–41].

The highest removal efficiency of Cr(VI) was identified in the pH range 5–6 which is in disagreement with results reported in the literature [38,42]. This may be explained by the main anion-exchange mechanism involved in the sorption of Cr(VI) on pine leaves [9]. Above pH 6, a decrease in Cr(VI) adsorption has been observed. This can be ascribed to the competition between the hydroxyl ions (OH^-) and Cr(VI) ions and the decrease in electrostatic attraction [4,43]. The pH_{pzc} of pine leaves was found to be 4.4. At pH lower than 4.4, pine leaves surface was positively charged favoring Cr(VI) sorption via electrostatic attraction with the negatively charged chromium species. For $pH > pH_{pzc}$ Cr(VI) sorption was not favored due to the electrostatic repulsion between the negatively charged chromium species and the negatively charged pine leaves surface.

3.3.2. Effect of adsorbent dose

The effect of adsorbent dose on Cr(VI) and Cu(II) adsorption was investigated varying the amount of adsorbent from 0.1 to 1.2 g per 40 mL of metal solution, at the initial metal concentration of 250 mg L^{-1}. The results are shown in Fig. 5b. The Cr(VI) removed from the solution increased from 30.1% to 99.9% with the increase in adsorbent dose from 0.1 to 1.2 g. The same behavior was observed with copper. The biosorbent dose increased the removal of Cu(II) from 28.1% to 98.4%. These results are due to the higher amount of adsorption sites in the biosorbent [44].

3.4. Adsorption isotherms

3.4.1. Effect of initial concentration

The effect of initial metal concentrations was investigated from 10 to 1,000 mg L^{-1}. The results are given in Fig. 5c and d. Fig. 5c shows that the metal ion adsorption increases sharply with the initial concentration until getting a maximum value. The increase of the metal concentration in the solution led to a higher concentration gradient between the solution and the biosorbent surface. This concentration gradient acts as a driving force for the transport of metal ions between the aqueous and the solid phase. Thus, the metal adsorption is enhanced until the saturation of the biosorbent [45,46]. However, the removal of metal from the solution decreased as the initial concentration of metal ion increased as shown in Fig. 5d. For instance, the removal of copper from the solution decreased from 98.3% to 27.1% when the initial metal concentration increased from 10 to 1,000 mg L^{-1} (Fig. 5d). At low metal concentrations, there are enough active binding sites on the biosorbent surface for the metal ions in solution. However, when the amount of metal ions in the liquid phase increases, the relative abundance of active sites in the biosorbent decreases, and hence, the fraction of metal removed from the liquid phase decreases.

3.4.2. Adsorption isotherm models

Isotherm models are a valuable tool for describing the interaction between the adsorbent and adsorbate. Four isotherm models namely: Langmuir, Freundlich, Temkin and Dubinin–Radushkevich, were used to fit the experimental adsorption data (Table 1, Fig. 6). Langmuir isotherm is based on the presumption of adsorption homogeneity [39]. It describes monolayer adsorption onto the surface of adsorbent, with no interaction between adsorbate molecules [37]. The non-linear Langmuir isotherm model can be written as Eq. (3).

$$q_e = \frac{\left(K_L q_{\max} C_e\right)}{\left(1 + K_L C_e\right)} \tag{3}$$

where q_e (mg g^{-1}) is the amount of metal ion adsorbed per unit mass of adsorbent, $q_{\max}$ is the maximum adsorption capacity (mg g^{-1}), C_e is the metal concentration in the liquid phase at the equilibrium (mg L^{-1}) and K_L is the Langmuir constant related to the energy of adsorption (L mg^{-1}).

The Langmuir isotherm is characterized by a dimensionless constant called equilibrium parameter R_L used to predict the affinity between the adsorbate and adsorbent. This parameter is calculated with Eq. (4):

$$R_L = \frac{1}{\left(1 + K_L C_0\right)} \tag{4}$$

Based on the value of R_L, the nature of adsorption could be either unfavorable ($R_L > 1$), linear ($R_L = 1$), favorable ($0 < R_L < 1$) or irreversible ($R_L = 0$) [46].

Freundlich isotherm assumes the multilayer sorption of adsorbate in heterogeneous surfaces, with sites with different energies involved in the adsorption process [37,47]. Eq. (5) shows the non-linearized from of the Freundlich isotherm.

$$q_e = K_F C_e^{1/n} \tag{5}$$

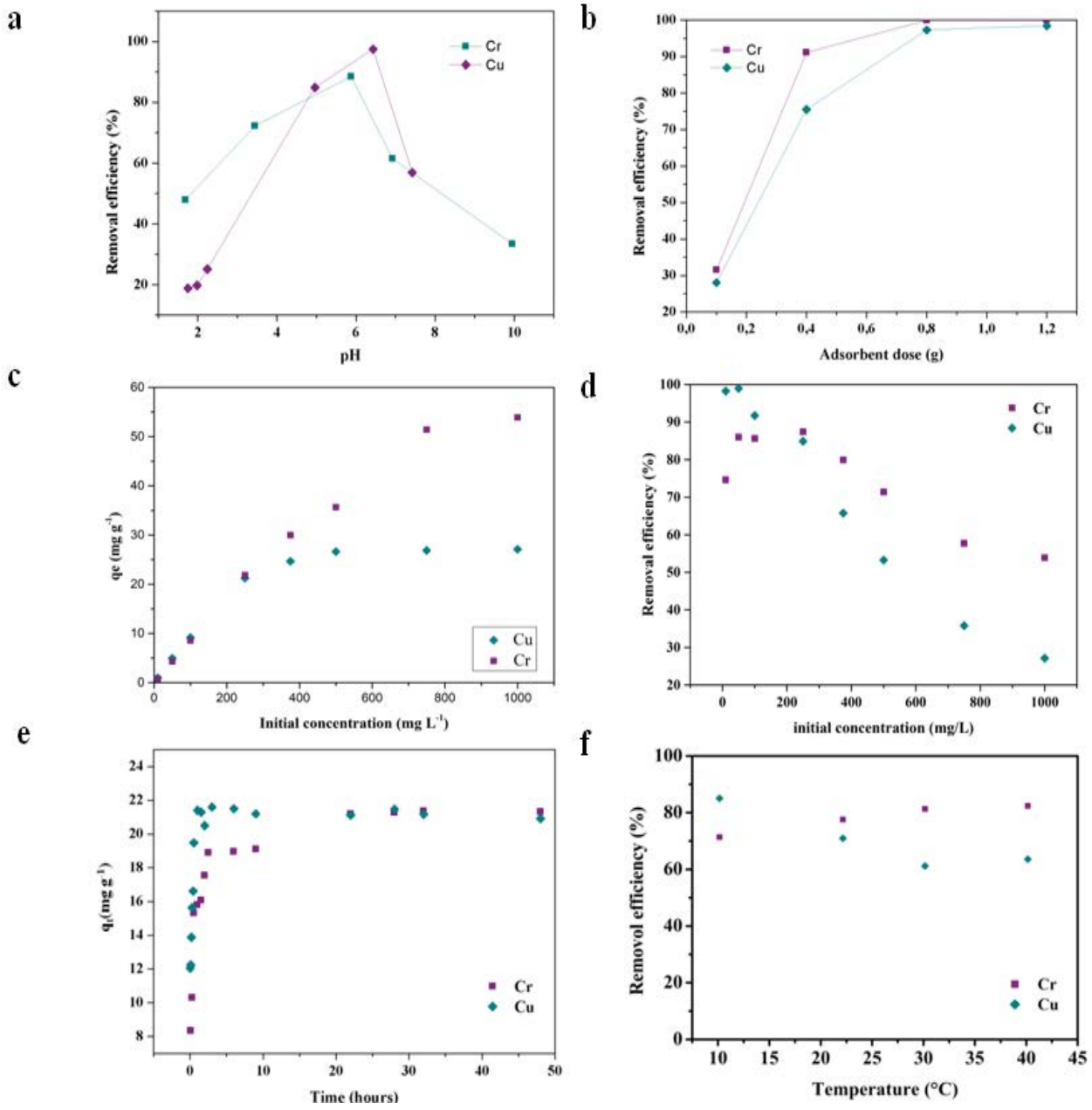

Fig. 5. Effects of pH (a), adsorbent dose (b), initial concentration (c and d), (e) contact time and temperature (f) on the adsorption of copper and chromium on pine cones and leaves respectively for an initial concentration of 250 mg L^{-1}.

where q_e is the equilibrium adsorption capacity (mg g^{-1}), K_F is the Freundlich isotherm constants related to adsorption capacity, and n is the adsorption intensity.

The Temkin isotherm model is represented by Eq. (6). This model assumes that the adsorption energy decreases linearly with the surface coverage [48].

$$q_e = \frac{RT}{b_T \ln\left(A_t C_e\right)} \tag{6}$$

where $B = RT/b_T$, b_T expressed as J mol^{-1}, is the Temkin constant related to the heat of adsorption. R is the universal gas constant (8.314 J mol^{-1} K^{-1}), T (K) is the absolute temperature and A_t (L mg^{-1}) is the equilibrium binding constant corresponding to the maximum binding energy.

The last isotherm model evaluated was proposed by Dubinin–Radushkevich [Eq. (7)]. This model describes an adsorption process with a Gaussian energy distribution onto heterogeneous surface [49].

$$q_e = q_D \exp\left(-\beta\, \varepsilon^2\right) \tag{7}$$

where q_D is the Dubinin–Radushkevich constant (mg g^{-1}), β is the constant related to the free energy and ε the Polanyi potential which is defined as $\varepsilon = RT \ln(1 + 1/C_e)$. The sorption energy E was calculated using Eq. (8).

$$E = \frac{1}{\sqrt{2\beta}} \quad (8)$$

The E (kJ mol^{-1}) value provides information about the nature of adsorption. If E lies between 8 and 16 kJ mol^{-1}, the sorption process is considered chemisorption, whereas if E < 8 kJ mol^{-1}, the sorption process is considered physisorption [50].

As it can be seen in Table 1, Langmuir model shows the highest correlation coefficient R^2 among the four isotherm models for Cu(II) in pine cones and Cr(VI) in pine leaves. Values of R_L ranging between 0 and 1 (R_L = 0.052 for Cu(II), and R_L = 0.24) indicating that the adsorption was favorable. Freundlich, Temkin and Dubinin–Radushkevich showed R^2 values lower than that for Langmuir model, suggesting that the latter fitted better the experimental data and that the adsorption process of Cr(VI) and Cu(II) onto pine wastes was a monolayer sorption without interaction between adsorbate molecules.

Table 1
Adsorption kinetics and equilibrium isotherms constants of the biosorption of Cu(II) on pine cones and Cr(VI) on pine leaves

Isotherm model	Parameters	Heavy metals	
		Cu(II)	Cr(VI)
Langmuir	K_L (L mg^{-1})	0.07	0.01
	q_{max} (mg g^{-1})	27.78	64.04
	R^2	0.973	0.976
Freundlich	K_F (mg$^{(1-1/n)}$ L$^{1/n}$ g^{-1})	7.60	3.95
	n	4.72	2.26
	R^2	0.881	0.930
Temkin	A_T (L mg^{-1})	6.70	0.24
	b_T (J mol^{-1})	0.73	0.22
	R^2	0.950	0.948
Dubinin–Radushkevich	q_D (mg g^{-1})	25.67	45.71
	E (kJ mol^{-1})	0.19	0.06
	R^2	0.943	0.863
Kinetic model			
Pseudo-first-order	q_e (mg g^{-1})	21.25	19.50
	k_1 (min^{-1})	0.10	0.05
	R^2	0.810	0.743
Pseudo-second-order	q_e (mg g^{-1})	21.93	20.65
	k_2 (g mg^{-1} min^{-1})	0.009	0.004
	R^2	0.942	0.914
Intraparticle diffusion	C (mg g^{-1})	5.15	17.07
	k_{id} (mg L$^{-1/2}$ min$^{-1/2}$)	2.89	0.092
	R^2	0.989	0.910

3.5. Adsorption kinetics

3.5.1. Effect of contact time

The effect of contact time on the biosorption of Cu(II) and Cr(VI) was studied up to 48 h at the initial metal concentration of 250 mg L^{-1}. The temperature was 20°C and the adsorbent dose was 0.4 g. As shown in Fig. 5e, the amount of adsorbed metal increased with the contact time. The adsorption rate was faster in the beginning of the test, when all the active sites are vacant, and then the adsorption rate decreases with the contact time. For example, in 30 min, the adsorbed amount was 19.4 mg g^{-1} for Cu(II), and 15.3 mg g^{-1} for Cr(VI). In 90 min, the adsorbed amount only increased up to 21.3 mg g^{-1} for Cu, and 16.07 mg g^{-1} for Cr(VI). This is due to the reduced fraction of vacant sites in the biosorbent surface as the adsorption progressed [21].

3.5.2. Kinetic study

Kinetic experimental data were fitted to the pseudo-first-order, pseudo-second-order, and intraparticle diffusion models (Fig. 7a–c) to investigate the possible adsorption mechanism and the rate controlling step in the adsorption of Cu(II) and Cr(VI) in pine cones and leaves. The pseudo-first-order equation (Lagergren's equation)

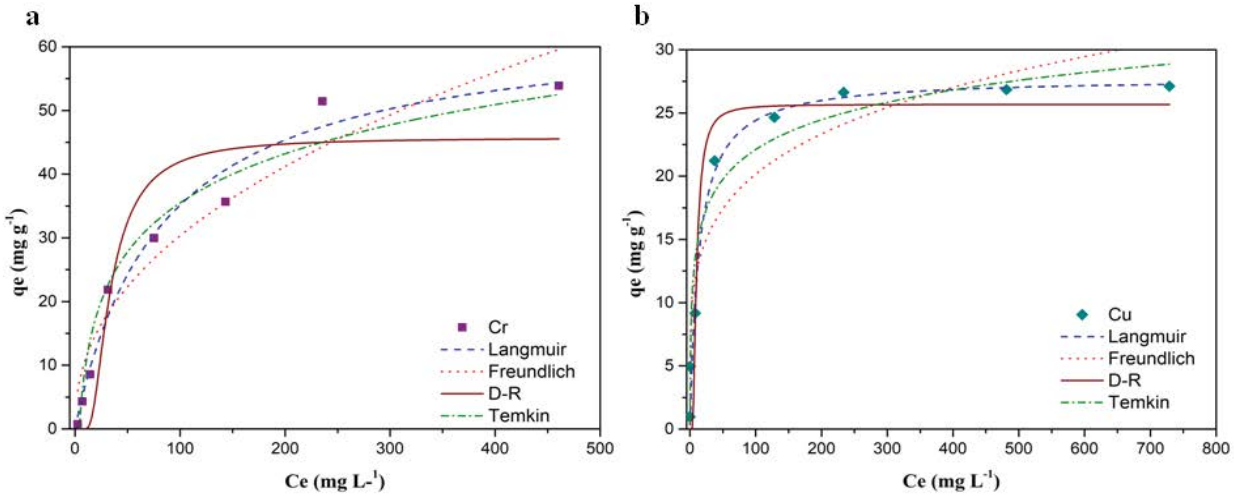

Fig. 6. Fitting curves of Langmuir, Freundlich, Temkin and Dubinin–Radushkevich isotherm models: (a) Cr(VI) and (b) Cu(II).

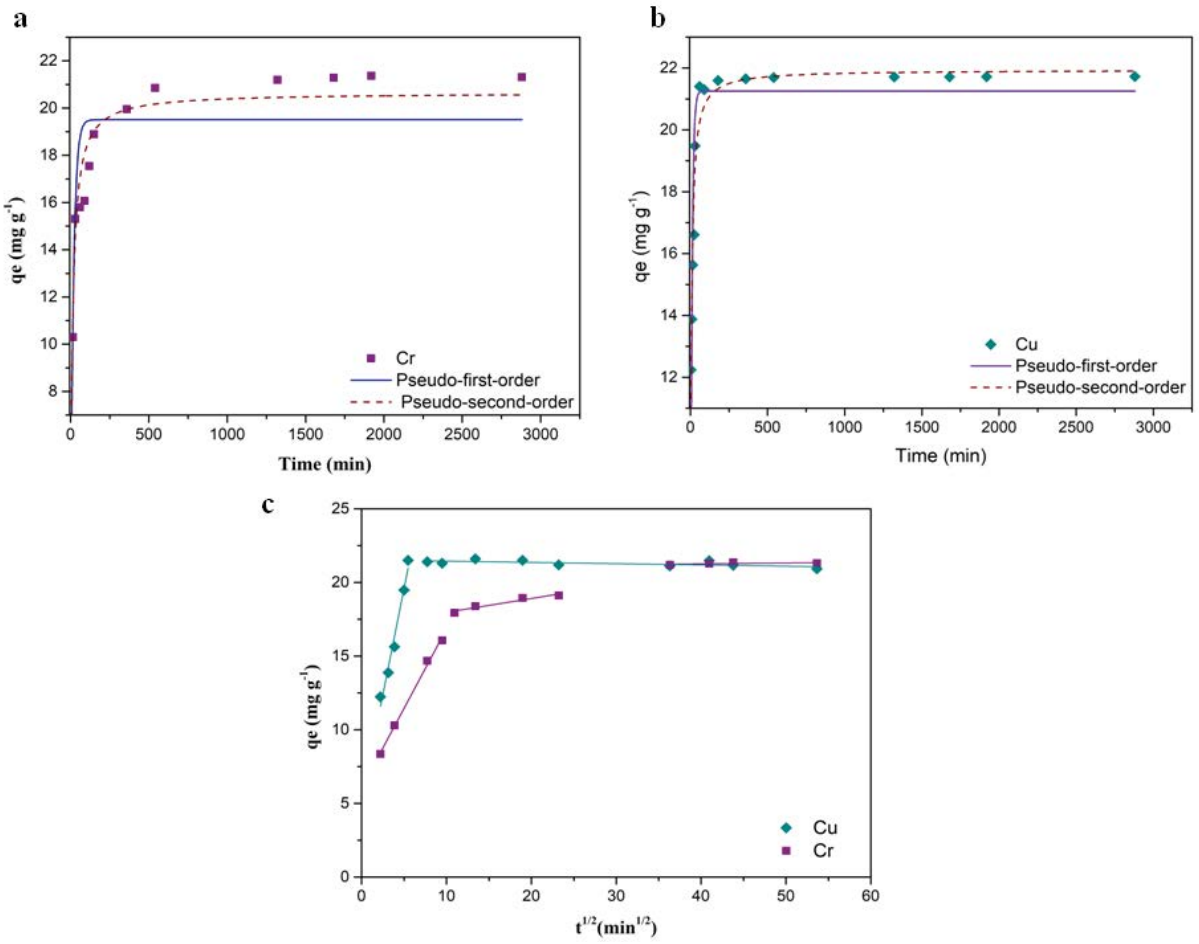

Fig. 7. Kinetic models: (a) pseudo-first-order, pseudo-second-order models for Cr(VI) sorption, (b) pseudo-first-order, pseudo-second-order models for Cu sorption and (c) intraparticle diffusion models for the adsorption of Cu and Cr(VI) onto pine cones and leaves respectively.

describes the adsorption of a liquid-solid system on the basis of adsorbent capacity. It suggests that one metal ion react with one sorption site on the surface of the adsorbent [51]. The Lagergren model and its integrated form can be expressed by Eqs. (9) and (10).

$$q_t = q_e\left(1-\exp\left(-k_1 t\right)\right) \tag{9}$$

$$\log\left(q_e - q_t\right) = \log\left(q_e\right) - \left(\frac{k_1}{2.303}\right)t \tag{10}$$

where k_1 is the pseudo-first-order rate constant of adsorption (min^{-1}), q_e is the amount of metal ion adsorbed in the equilibrium, and q_t (mg g^{-1}) is the metal adsorbed at any time t (min).

The pseudo-second-order kinetic model can be expressed by Eqs. (11) and (12).

$$q_t = \frac{t}{\left(t/k_2 q_e^{\,2}\right)} + \left(\frac{t}{q_e}\right) \tag{11}$$

$$\frac{t}{q_t} = \frac{1}{k_2 q_e^2} + \frac{1}{q_e} \tag{12}$$

where k_2 is the pseudo-second-order adsorption rate constant (g mg^{-1} min^{-1}).

Table 1 shows the parameters for each kinetic model and the correlation coefficient R^2. The pseudo-second-order kinetic model correlates better the experimental data (R^2 values of pseudo-second-order model (Cu(II):0.942, Cr(VI): 0.914) were higher the R^2 values of pseudo-first-order model (Cu(II):0.810, Cr(VI): 0.743). Moreover, the $q_{e(cal)}$ values calculated from the pseudo-second-order model were in good agreement with experimental values of $q_{e(exp)}$ (21.62 mg g^{-1} for Cu(II) and 21.36 mg g^{-1} for Cr(VI)); whereas the pseudo-first-order kinetic model predicts lower values.

The Weber–Morris intraparticle diffusion model was used to investigate the diffusion mechanism in the porous structure of the adsorbent, and its influence in the adsorption rate. The intraparticle diffusion model equation is expressed by Eq. (13).

$$q_t = k_{id} t^{1/2} + C \tag{13}$$

where k_{id} is the intraparticle diffusion rate constant (mg g^{-1} $min^{1/2}$) and C is the value of intercept in a plot of q_t vs. $t^{1/2}$ [52].

The linearity of the plot q_t vs. $t^{1/2}$ informs about the diffusion mechanism. If the plot is linear and passes through the origin, then the intraparticle diffusion is the only rate limiting step. A multiple linear plot suggests that the adsorption process is governed by more than one step [49,53,54]. The plots q_t vs. $t^{1/2}$ for the adsorption of Cu/pine cones or Cr/pine leaves (Fig. 7c) showed a multilinear plot suggesting that the intraparticle diffusion was not the only rate limiting step. As depicted in Fig. 7c, chromium adsorption process occurred in three phases. The first linear segment indicates surface or film diffusion rate control, the second linear segment represents a gradual biosorption where pore or intraparticle diffusion were rate limiting step, and the third segment is the final equilibrium. Fig. 7c shows that copper adsorption took place on two steps. The first step corresponded the intraparticle diffusion. The second step was attributed to the final equilibrium stage [21]. The intra-particle rate constant k_{id} and intercept C are given in Table 1. The value of C describes the boundary layer effect. The larger the intercept value the greater the boundary layer effect [54]. For both Cu(II) and Cr(VI), C values were different from 0, meaning that the intraparticle diffusion is not the exclusive rate controlling step [4,39].

3.6. Effect of temperature and thermodynamic study

The effect of temperature was investigated over the range of 10°C–40°C and the results are shown in Fig. 5f. As can be seen, the biosorption rate of copper decreased from 85.0% to 61.2% by increasing the temperature from 10°C to 30°C. These results suggest the exothermic nature of biosorption process. The decrease in adsorption at higher temperature was explained by the weakening of supportive forces between active sites on the adsorbent and Cu(II) ions. This decrease in adsorption capacity with increase in temperature is known to be due to the enhancement of the desorption step in the sorption mechanism [37]. However, different behavior was observed with Cr(VI) since the removal efficiency increased from 71.4% to 82.4% with the increase in solution temperature from 10°C to 40°C, indicating the endothermic nature of Cr(VI) adsorption in pine leaves. The increase in biosorption rate with the temperature can be attributed to the enhanced mobility of Cr(VI) in solution [42].

The free energy change, enthalpy and entropy were evaluated using Eqs. (14)–(16) [39]:

$$\Delta G^\circ = -RT\ \ln K_c \tag{14}$$

$$\ln K_c = \frac{\Delta S^\circ}{R} - \frac{\Delta H^\circ}{RT} \tag{15}$$

$$K_c = \frac{C_s}{C_e} \tag{16}$$

where ΔG° is the free energy change, R is the universal gas constant, T is the absolute temperature (K), K_c represents the equilibrium constant for adsorption, C_s is the metal concentration in the solid phase in equilibrium (mg L^{-1}) with the metal concentration in solution, C_e (mg L^{-1}). ΔH° is the enthalpy change (kJ mol^{-1}), ΔS° is the entropy change (kJ mol^{-1} K^{-1}). Enthalpy and entropy are determined from the slope and intercept plotting $\ln K_c$ vs. $1/T$ (Fig. S2).

The thermodynamic parameters of chromium and copper adsorption on pine leaves and cones were determined and listed in Table 2. The positive value of ΔH° confirmed the endothermic nature of chromium biosorption process, and the positive value of ΔS° also suggested the increase of randomness at the solid-solution interface [42].The exothermic nature of copper biosorption was confirmed by the negative value of ΔH°. The negative value of ΔS° suggested the decrease of randomness at the solid-solution interface as result of Cu(II) adsorption in pine cones [37]. Houhoune et al. [55] reported that the negative ΔS_{ads} value suggests that release of water from the firmly bound hydration of Na+ contributes to the exchange process as it moves from adsorbent to solution phase. Krobba et al. [56] have also reported that a negative activation entropy ΔS^* value reflects that no significant change occurs in the internal structure of the adsorbent NaY during the adsorption of Cu^{2+} ions.

3.7. Desorption and reuse study

The regeneration and the reuse of biomass are of key importance in any large scale application of metal removal from wastewater. Desorption of metals and possible reuse of the biomass for further metal adsorption was studied. The desorption experiments were conducted with five solvents/solutions: deionized water, NaOH, HCl, HNO_3 and EDTA, at 20°C. Fig. 8a showed that nitric acid was the most efficient extractant for Cr (55.4%) after 2 cycles of desorption, followed by hydrochloric acid (38.3%), and EDTA (19.7%). Only 8.8% of chromium was released using NaOH. The Cr(VI) desorbed with water was negligible. These results confirm the stability of the metal adsorbed in the pine leaves at neutral or alkaline pH, and the necessity

Table 2
Thermodynamic parameters of the biosorption of Cu in pine cones and Cr in pine leaves

	Temperature (°C)	ΔG° (kJ mol^{-1})	ΔH° (kJ mol^{-1})	ΔS° (kJ mol^{-1} K^{-1})
Copper	10	–3.494	–29.61	–0.09
	20	–2.216		
	30	–1.679		
Chromium	10	–2.15	16.10	0.06
	20	–3.05		
	30	–3.70		
	40	–4.02		

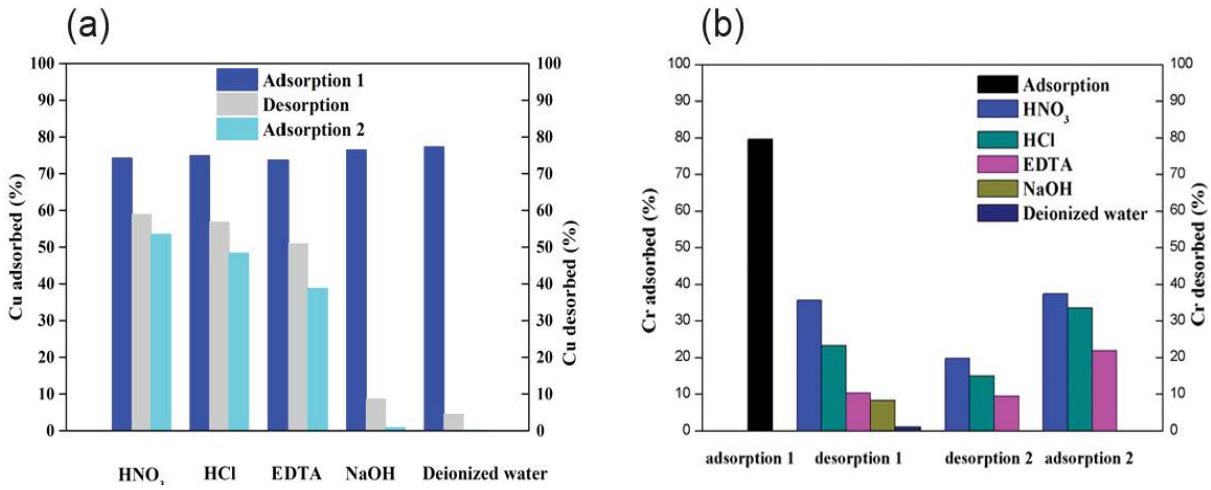

Fig. 8. Desorption/adsorption studies of (a) copper from pine cones and (b) chromium from pine leaves, at 20°C.

of an acid environment to mobilize the metal. The reuse of pine leaves for the adsorption of Cr(VI) showed 50% loss of capacity. Copper could also be removed for the pine cones (Fig. 8b), being HNO_3 the most efficient extractant (79.4% of Cu(II) was removed), followed by HCl (74.9% of Cu(II)) and EDTA (69.2% of Cu(II)).In this case, pine cones only showed a loss of adsorption capacity of about 25% for Cu(II). These results have an enormous interest for large scale application in real effluents.

4. Conclusions

The adsorption of Cr(VI) on pine leaves and Cu(II) on pine cones revealed that the pine waste materials are potentially suitable for the retention of these metals from aqueous solutions. pH, biosorbent dose, contact time and initial metal ion concentration affected the adsorption results. Complete adsorption of Cu and Cr was observed with 0.8 g of biosorbent and 40 mL of 250 mg L^{-1} of metal solution. The adsorption is very fast, and the equilibrium is reached in less than 1 h of contact. Langmuir model fitted the adsorption of Cr(VI) and Cu(II). The maximum adsorption of metals pine cones and leaves were found to be 27.78 mg g^{-1} for Cu and 64.04 mg g^{-1} for Cr(VI). Analysis of kinetic data showed that the adsorption process followed the pseudo-second-order model for both metals. The thermodynamic study confirmed that the adsorption of Cu(II) in pine cones was exothermic whereas Cr(VI) adsorption in pine leaves was endothermic. The desorption of the metals with nitric acid allowed for the reuse of the biosorbent although a significant loss of adsorption capacity in the reused biomass was observed. Overall, it can be concluded that pine waste materials (cones and leaves) were an effective eco-friendly biosorbent for the removal of copper and chromium from wastewaters.

Symbols

T	—	Definition, Units
A_t	—	Equilibrium binding constant for the maximum binding energy, L mg^{-1}
b_T	—	Heat biosorption constant, J mol^{-1}
C	—	Value of the intercept of the plot q_t vs. $t^{1/2}$, mg g^{-1}
C_0	—	Initial metal concentration in the liquid phase, mg L^{-1}
C_e	—	Metal concentration in the liquid-phase in the equilibrium, mg L^{-1}
C_s	—	Metal concentration in the solid phase in equilibrium, mg L^{-1}
E	—	Sorption energy, kJ mol^{-1}
k_1	—	Pseudo-first-order rate coefficient of adsorption, min^{-1}
k_2	—	Pseudo-second-order rate coefficient of adsorption, g mg^{-1} min^{-1}
K_d	—	Equilibrium constant for adsorption, –
k_{id}	—	Intraparticle diffusion rate constant, mg g^{-1} $min^{1/2}$
K_F	—	Freundlich isotherm constant related to adsorption capacity, $mg^{(1-1/n)}$ $L^{1/n}$ g^{-1}
K_L	—	Langmuir constant related to energy of adsorption, L mg^{-1}
n	—	Adsorption intensity (Freundlich isotherm), –
q_D	—	Dubinin–Radushkevich constant, mg g^{-1}
q_e	—	Metal adsorbed in the equilibrium (adsorption capacity), mg g^{-1}
q_{max}	—	Maximum adsorption capacity, mg g^{-1}
q_t	—	Metal adsorbed at any time (adsorption capacity), mg g^{-1}
R	—	Theideal gas constant (8.314), J mol^{-1} K^{-1}
R^2	—	Correlation coefficient, –
R_L	—	Equilibrium parameter (Langmuir isotherm), –
T	—	Time, min
T	—	Absolute temperature, K
V	—	Volume of liquid phase, L
W	—	Adsorbent dose, G
B	—	Constant related to the free energy, mol^2 kJ^{-2}
$\Delta H°$	—	Enthalpy change, kJ mol^{-1}
$\Delta G°$	—	Free energy change, kJ mol^{-1}
$\Delta S°$	—	Entropy change, kJ mol^{-1} K^{-1}
ε	—	Polanyi potential, –

References

[1] L. Khezami, R. Capart, Removal of chromium(VI) from aqueous solution by activated carbons: kinetic and equilibrium studies, J. Hazard. Mater., 123 (2005) 223–231.

[2] I. Anastopoulos, G.Z. Kyzas, Composts as biosorbents for decontamination of various pollutants: a review, Water Air Soil Pollut., 226 (2015) 61, doi: 10.1007/s11270-015-2345-2.
[3] A.Ş. Yargıç, R.Z. Yarbay Şahin, N. Özbay, E. Önal, Assessment of toxic copper(II) biosorption from aqueous solution by chemically-treated tomato waste, J. Cleaner Prod., 88 (2015) 152–159.
[4] R. Khosravi, G. Moussavi, M.T. Ghaneian, M.H. Ehrampoush, B. Barikbin, A.A. Ebrahimi, G. Sharifzardeh, Chromium adsorption from aqueous solution using novel green nano-composite: adsorbent characterization, isotherm, kinetic and thermodynamic investigation, J. Mol. Liq., 256 (2018) 163–174.
[5] X. Liu, Z.Q. Chen, B. Han, C.L. Su, Q. Han, W.Z. Chen, Biosorption of copper ions from aqueous solution using rape straw powders: optimization, equilibrium and kinetic studies, Ecotoxicol. Environ. Saf., 150 (2018) 251–259.
[6] W.S.W. Ngah, M.A.K.M. Hanafiah, Removal of heavy metal ions from wastewater by chemically modified plant wastes as adsorbents: a review, Bioresour. Technol., 99 (2008) 3935–3948.
[7] Q.Q. Zhong, Q.Y. Yue, B.Y. Gao, Q. Li, X. Xu, A novel amphoteric adsorbent derived from biomass materials: synthesis and adsorption for Cu(II)/Cr(VI) in single and binary systems, Chem. Eng. J., 229 (2013) 90–98.
[8] C. Sakulthaew, C. Chokejaroenrat, A. Poapolathep, T. Satapanajaru, S. Poapolathep, Hexavalent chromium adsorption from aqueous solution using carbon nano-onions (CNOs), Chemosphere, 184 (2017) 1168–1174.
[9] M. Khitous, Z. Salem, D. Halliche, Effect of interlayer anions on chromium removal using Mg–Al layered double hydroxides: kinetic, equilibrium and thermodynamic studies, Chin. J. Chem. Eng., 24 (2016) 433–445.
[10] S. Rangabhashiyam, P. Balasubramanian, Characteristics, performances, equilibrium and kinetic modeling aspects of heavy metal removal using algae, Bioresour. Technol. Rep., 5 (2019) 261–279.
[11] F.M. Pellera, A. Giannis, D. Kalderis, K. Anastasiadou, R. Stegmann, J.Y. Wang, E. Gidarakos, Adsorption of Cu(II) ions from aqueous solutions on biochars prepared from agricultural by-products, J. Environ. Manage., 96 (2012) 35–42.
[12] N.G. Turan, S. Elevli, B. Mesci, Adsorption of copper and zinc ions on illite: determination of the optimal conditions by the statistical design of experiments, Appl. Clay Sci., 52 (2011) 392–399.
[13] S.H. Lin, R.S. Juang, Removal of free and chelated Cu(II) ions from water by a nondispersive solvent extraction process, Water Res., 36 (2002) 3611–3619.
[14] A.I. Zouboulis, K.A. Matis, B.G. Lanara, C.L. Neskovic, Removal of cadmium from dilute solutions by hydroxyapatite. II. Flotation studies, Sep. Sci. Technol., 32 (1997) 1755–1767.
[15] I. Gajda, A. Stinchcombe, J. Greenman, C. Melhuish, I. Ieropoulos, Microbial fuel cell – a novel self-powered wastewater electrolyser for electrocoagulation of heavy metals, Int. J. Hydrogen Energy, 42 (2017) 1813–1819.
[16] C. Feng, N. Sugiura, S. Shimada, T. Maekawa, Development of a high performance electrochemical wastewater treatment system, J. Hazard. Mater., 103 (2003) 65–78.
[17] S. Rengaraj, C.K. Joo, Y. Kim, J. Yi, Kinetics of removal of chromium from water and electronic process wastewater by ion exchange resins: 1200H, 1500H and IRN97H, J. Hazard. Mater., 102 (2003) 257–275.
[18] L. Canet, M. Ilpide, P. Seta, Efficient facilitated transport of lead, cadmium, zinc, and silver across a flat-sheet-supported liquid membrane mediated by lasalocid A, Sep. Sci. Technol., 37 (2002) 1851–1860.
[19] P. Arivalagan, D. Singaraj, V. Haridass, T. Kaliannan, Removal of cadmium from aqueous solution by batch studies using *Bacillus cereus*, Ecol. Eng., 71 (2014) 728–735.
[20] N.R. Ekere, A.B. Agwogie, J.N. Ihedioha, Studies of biosorption of Pb^{2+}, Cd^{2+} and Cu^{2+} from aqueous solutions using *Adansonia digitata* root powders, Int. J. Phytorem., 18 (2016) 116–125.
[21] S.H. Peng, R. Wang, L.Z. Yang, L. He, X. He, X. Liu, Biosorption of copper, zinc, cadmium and chromium ions from aqueous solution by natural foxtail millet shell, Ecotoxicol. Environ. Saf., 165 (2018) 61–69.
[22] F.A. Santos, L. Alban, C.L.C. Frankenberg, M. Pires, Characterization and use of biosorbents prepared from forestry waste and their washed extracts to reduce/remove chromium, Int. J. Environ. Sci. Technol., 13 (2016) 327–338.
[23] M.A. Hossain, H.H. Ngo, W.S. Guo, T. Setiadi, Adsorption and desorption of copper(II) ions onto garden grass, Bioresour. Technol., 121 (2012) 386–395.
[24] N.R. Bishnoi, M. Bajaj, N. Sharma, A. Gupta, Adsorption of Cr(VI) on activated rice husk carbon and activated alumina, Bioresour. Technol., 91 (2004) 305–307.
[25] K. Wilson, H. Yang, C.W. Seo, W.E. Marshall, Select metal adsorption by activated carbon made from peanut shells, Bioresour. Technol., 97 (2006) 2266–2270.
[26] R.S.D. Castro, L. Caetano, G. Ferreira, P.M. Padilha, M.J. Saeki, L.F. Zara, M.A.U. Martines, G.R. Castro, Banana peel applied to the solid phase extraction of copper and lead from river water: preconcentration of metal ions with a fruit waste, Ind. Eng. Chem. Res., 50 (2011) 3446–3451.
[27] T. Bohli, A. Ouederni, N. Fiol, I. Villaescusa, Evaluation of an activated carbon from olive stones used as an adsorbent for heavy metal removal from aqueous phases, C.R. Chim., 18 (2015) 88–99.
[28] M. Rafatullah, O. Sulaiman, R. Hashim, A. Ahmad, Adsorption of copper(II), chromium(III), nickel(II) and lead(II) ions from aqueous solutions by meranti sawdust, J. Hazard. Mater., 170 (2009) 969–977.
[29] E.B. Khalifa, B. Rzig, R. Chakroun, H. Nouagui, B. Hamrouni, Application of response surface methodology for chromium removal by adsorption on low-cost biosorbent, Chemom. Intell. Lab. Syst., 189 (2019) 18–26.
[30] D. Ferhat, D. Nibou, E.H. Mekatel, S. Amokrane, Adsorption of Ni2+ ions onto NaX and NaY zeolites: equilibrium, kinetic, intra crystalline diffusion and thermodynamic studies, Iran. J. Chem. Chem. Eng., 38 (2019) 63–81
[31] T. Akar, S. Tunali, Biosorption characteristics of *Aspergillus flavus* biomass for removal of Pb(II) and Cu(II) ions from an aqueous solution, Bioresour. Technol., 97 (2006) 1780–1787.
[32] S. Liang, X. Guo, N. Feng, Q. Tian, Adsorption of Cu^{2+} and Cd^{2+} from aqueous solution by mercapto-acetic acid modified orange peel, Colloids Surf., B, 73 (2009) 10–14.
[33] M.M. Areco, S. Hanela, J. Duran, M.D.S. Afonso, Biosorption of Cu(II), Zn(II), Cd(II) and Pb(II) by dead biomasses of green alga *Ulva lactuca* and the development of a sustainable matrix for adsorption implementation, J. Hazard. Mater., 213–214 (2012) 123–132.
[34] S.B. Ali, I. Jaouali, S.S. Najar, A. Ouederni, Characterization and adsorption capacity of raw pomegranate peel biosorbent for copper removal, J. Cleaner Prod., 142 (2017) 3809–3821.
[35] S.S. Baral, S.N. Das, P. Rath, Hexavalent chromium removal from aqueous solution by adsorption on treated sawdust, Biochem. Eng. J., 31 (2006) 216–222.
[36] V.K. Gupta, A. Rastogi, A. Nayak, Adsorption studies on the removal of hexavalent chromium from aqueous solution using a low cost fertilizer industry waste material, J. Colloid Interface Sci., 342 (2010) 135–141.
[37] M. Akram, H.N. Bhatti, M. Iqbal, S. Noreen, S. Sadaf, Biocomposite efficiency for Cr(VI) adsorption: kinetic, equilibrium and thermodynamics studies, J. Environ. Chem. Eng., 5 (2017) 400–411.
[38] M. Kumar, A. Pal, J. Singh, S. Garg, M. Bala, A. Vyas, Y.P. Khasa, U.C. Pachouri, Removal of chromium from water effluent by adsorption onto *Vetiveria zizanioides* and *Anabaena* species, Nat. Sci., 5 (2013) 341, doi: 10.4236/ns.2013.53047.
[39] V. Manirethan, K. Raval, R. Rajan, H. Thaira, R.M. Balakrishnan, Kinetic and thermodynamic studies on the adsorption of heavy metals from aqueous solution by melanin nanopigment obtained from marine source: *Pseudomonas stutzeri*, J. Environ. Manage., 214 (2018) 315–324.
[40] A. Aid, S. Amokrane, D. Nibou, E. Mekatel, M. Trari, V. Hulea, Modeling biosorption of Cr(VI) onto *Ulva compressa* L. from aqueous solutions, Water. Sci. Technol., 77 (2018) 60–69.

[41] S. Ladjali, S. Amokrane, E.H. Mekatel, D. Nibou, Adsorption of Cr(VI) on *Stipa tenacissima* L (Alfa): characteristics, kinetics and thermodynamic studies, Sep. Sci. Technol., 54 (2019) 876–887.
[42] U. Tyagi, V. Khandegar, Biosorption potential of *Vetiveria zizanioides* for the removal of chromium(VI) from synthetic wastewater, J. Hazard. Toxic Radioact. Waste, 22 (2018) 04018014, doi: 10.1061/(ASCE)HZ.2153-5515.0000403.
[43] J. Yang, M. Yu, W. Chen, Adsorption of hexavalent chromium from aqueous solution by activated carbon prepared from longan seed: kinetics, equilibrium and thermodynamics, J. Ind. Eng. Chem., 21 (2015) 414–422.
[44] K.V. Kumar, K. Porkodi, Mass transfer, kinetics and equilibrium studies for the biosorption of methylene blue using *Paspalum notatum*, J. Hazard. Mater., 146 (2007) 214–226.
[45] Y.A. Yahaya, M.M. Don, S. Bhatia, Biosorption of copper(II) onto immobilized cells of *Pycnoporus sanguineus* from aqueous solution: equilibrium and kinetic studies, J. Hazard. Mater., 161 (2009) 189–195.
[46] A. Jain, M. Agarwal, Kinetic equilibrium and thermodynamic study of arsenic removal from water using alumina supported iron nanoparticles, J. Water Process Eng., 19 (2017) 51–59.
[47] H.I. Chieng, L.B.L. Lim, N. Priyantha, Enhancing adsorption capacity of toxic malachite green dye through chemically modified breadnut peel: equilibrium, thermodynamics, kinetics and regeneration studies, Environ. Technol., 36 (2015) 86–97.
[48] H.K. Boparai, M. Joseph, D.M. O'Carroll, Kinetics and thermodynamics of cadmium ion removal by adsorption onto nano-zerovalent iron particles, J. Hazard. Mater., 186 (2011) 458–465.
[49] A.O. Dada, A.P. Olalekan, A.M. Olatunya, O. Dada, Langmuir, Freundlich, Temkin and Dubinin–Radushkevich isotherms studies of equilibrium sorption of Zn^{2+} unto phosphoric acid modified rice husk, IOSR J. Appl. Chem., 3 (2012) 38–45.
[50] B. Das, N.K. Mondal, R. Bhaumik, P. Roy, K.C. Pal, C.R. Das, Removal of copper from aqueous solution using alluvial soil of Indian origin: equilibrium, kinetic and thermodynamic study, J. Mater. Environ. Sci., 4 (2013) 392–408.
[51] S. Lagergren, Zurtheorie der sogenannten adsorption gelosterstoffe, KungligaSvenskaVetenskapsakademiens, Handlingar, 24 (1898) 1–39.
[52] I.A.W. Tan, A.L. Ahmad, B.H. Hameed, Adsorption of basic dye on high-surface-area activated carbon prepared from coconut husk: equilibrium, kinetic and thermodynamic studies, J. Hazard. Mater., 154 (2008) 337–346.
[53] S.I.H. Taqvi, S.M. Hasany, M.I. Bhanger, Sorption profile of Cd(II) ions onto beach sand from aqueous solutions, J. Hazard. Mater., 141 (2007) 37–44.
[54] Y. Khambhaty, K. Mody, S. Basha, B. Jha, Kinetics, equilibrium and thermodynamic studies on biosorption of hexavalent chromium by dead fungal biomass of marine *Aspergillus niger*, Chem. Eng. J., 145 (2009) 489–495.
[55] F. Houhoune, D. Nibou, S. Amokrane, M. Barkat, Modelling and adsorption studies of removal uranium(VI) ions on synthesized zeolite NaY, Desal. Water Treat., 51 (2013) 5583–5591.
[56] A. Krobba, D. Nibou, S. Amokrane, H. Mekatel, Adsorption of copper(II) onto molecular sieves NaY, Desal. Water Treat., 37 (2012) 1–7.

Supporting information

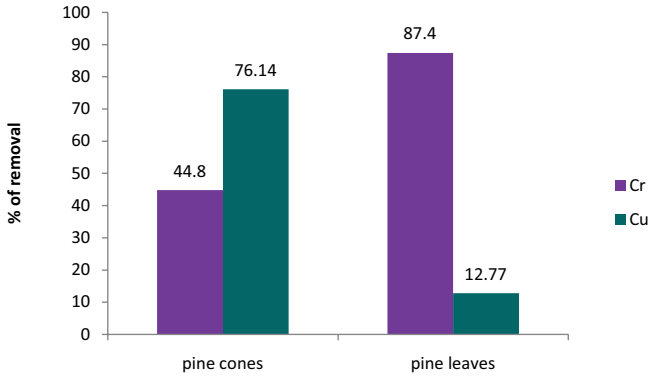

Fig. S1. Selection of the adsorbent for copper and chromium removal.

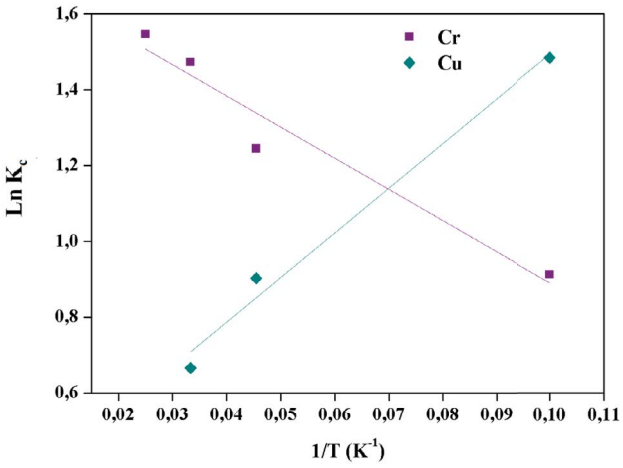

Fig. S2. Plot of lnK_c vs. 1/T.